

Cite this: *Phys. Chem. Chem. Phys.*, 2012, **14**, 10882–10885

www.rsc.org/pccp

On the pathway of photoexcited electrons: probing photon-to-electron and photon-to-phonon conversions in silicon by ATR-IR†

Engin Karabudak,^{*ab} Emre Yüce,^c Stefan Schlautmann,^a Ole Hansen,^d Guido Mul^e and Han (J.G.E.) Gardeniers^{ab}

Received 14th April 2012, Accepted 22nd June 2012

DOI: 10.1039/c2cp41831b

Photoexcitation and charge carrier thermalization inside semiconductor photocatalysts are two important steps in solar fuel production. Here, photoexcitation and charge carrier thermalization in a silicon wafer are for the first time probed by a novel, yet simple and user-friendly Attenuated Total Reflectance Infrared spectroscopy (ATR-IR) system.

It has been argued for a long time now that an energy crisis may be at hand, due to the predicted increase of energy demands in the near future.¹ As a solution to a future energy shortage, solar fuel, *i.e.* a fuel originating from sunlight, has been mentioned as one of the possible candidates,^{2,3} as long as it may be produced globally. Cost efficient global solar fuel production is only possible with devices that are cheap, efficient and stable. In terms of stability, semiconductor-based photocatalysis³ is an appealing possible solution. When the past forty years are considered, semiconductor photocatalyst⁴ synthesis research has been dedicated to the development of stable, cheap and efficient materials that can produce solar fuel, however without truly groundbreaking success. One reason for this in our view is, apart from the high complexity of the problem, the lack of a simple and easy to use characterization technique that, in addition to the many characterization techniques available nowadays that focus on probing chemical reactions on the surface of the material, can also probe processes inside the semiconductor. In order to exploit other directions for success in terms of efficiency, what is especially required is a simple and easy to use technique to probe both photon-to-electron and photon-to-phonon conversions inside the semiconductor.

Attenuated Total Reflectance Infrared (ATR-IR)⁵ spectroscopy is a relatively simple surface technique which is heavily used daily by synthetic chemists. ATR is also well-known for probing chemical reactions on a photocatalyst surface, which provides valuable information needed to understand how photons are converted to fuel. If one looks in more detail at such a process, it becomes clear that semiconductor photocatalysts convert the energy of photons into a fuel in four steps.⁴ The first step is photoabsorption in which any photon that has an energy higher than the band gap of the semiconductor (above-band-gap photon) causes an excited state. In this step, if the photon is absorbed by the semiconductor, one hundred percent of the photon energy is transferred to an excited electron.⁶ With this energy, the electron is excited from the valence band to the conduction band. The second step is thermalization,⁶ in which some portion of this energy (excess energy of the electron above the band gap) is wasted as lattice vibrations. This second step is important because this step puts a theoretical limit on efficiency not only for solar fuel production but also for photovoltaic cells. The third step is transportation of electrons and holes to the surface of the semiconductor, followed by the fourth step which is the chemical reaction, involving electron transfer reactions, at the surface. To obtain real success in solar to fuel conversion, all the aforementioned steps need to be probed experimentally. Indeed, probing dynamics of photoexcitation and thermalization is not easy and requires time-resolved spectroscopy^{7–9} with a precise optical bench with transmission or reflection configurations, which often is too expensive and complex for everyday use in a synthetic chemistry lab.

Previously, the fate of photoexcited carriers has been studied on TiO_x nanoparticle thin films using ATR-IR.^{10,11} However, there is no reported ATR-IR work on two-photon excited free carriers in Si that reveals the thermalization inside a single crystal semiconductor, which is the method we propose in this paper. An unique property of our system is that, thanks to the possibilities that silicon micromachining offers, and the use of a four-mirror holder, we can use thin (530 μm or less) silicon crystals, whereas most commercial systems are much thicker (1 mm). The use of thinner silicon specimens has two major advantages: firstly, the material is thinner than the penetration depth of the light at the wavelength of our laser (for 1064 nm photons, the penetration depth is about 0.99 mm, see ESI† for calculations),

^a Mesoscale Chemical Systems Group, University of Twente, P.O. Box 217, 7500 AE Enschede, The Netherlands. E-mail: e.karabudak@utwente.nl; Fax: +31 (0)53-4894683; Tel: +31(0)53-489 25 940

^b BioSolar Cells, P.O. Box 98, 6700 AB Wageningen, The Netherlands

^c Complex Photonic Systems (COPS), MESA+ Institute for Nanotechnology, P.O. Box 217, 7500 AE Enschede, The Netherlands

^d Department of Micro- and Nanotechnology and CINF, Building 345E, DTU, DK-2800 Lyngby, Denmark

^e Photo Catalytic Synthesis Group, MESA+ Institute for Nanotechnology, Enschede, The Netherlands

† Electronic supplementary information (ESI) available. See DOI: 10.1039/c2cp41831b

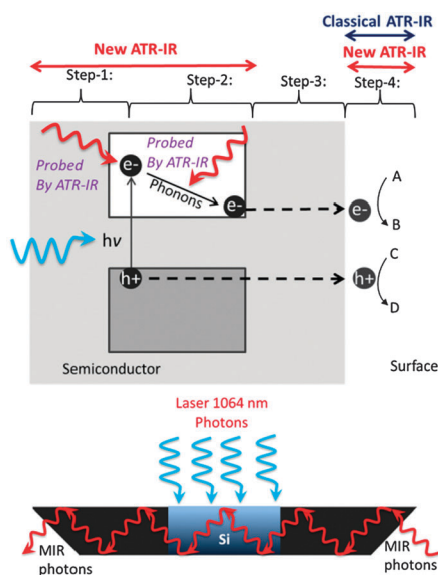


Fig. 1 (a) Schematic showing the steps of solar to fuel conversion in a semiconductor photocatalyst; (b) novel ATR-IR setup introduced in this paper.

which means that the entire bulk of the silicon crystal is exposed to the photons. Therefore, the attenuated IR light overlaps better with photoexcited electrons inside the silicon wafer. As a result of this, we increase the probability of creating two-photon excited carriers which allows us to investigate free carrier and phonon interactions. Secondly, it is well known that phonon absorption intensities decrease with the thickness of the silicon crystal.¹⁰ Consequently, the cut off wavenumber⁵ of 1500 cm^{-1} , which is well-known for silicon ATR crystals, now reduces to 1200 cm^{-1} which is a unique property^{11,12} of our setup and also not possible with commercial crystals. With this lower cut off wavenumber, phonons can be detected without the need for more expensive time resolved spectroscopy or the like.

Our ATR-IR setup is composed of four mirrors, a silicon crystal, a continuous-wave portable laser and an IR spectrometer which has its own mid-infrared (MIR) photon source (Fig. 1). State-of-the-art silicon microfabrication was used to etch two sides of a CZ silicon wafer ($2\text{ cm} \times 1.5\text{ cm} \times 530\text{ }\mu\text{m}$) with KOH to construct an ATR-IR silicon crystal as described before.^{11,12} A four mirror holder was designed and constructed to couple IR light into the crystal^{11,12} using a commercial IR spectrometer (Vertex 70, Bruker Optics) to determine IR spectra. During acquisition of an IR spectrum, a continuous-wave portable laser (Casix Nd-YAG laser, 130 mW, 1064 nm) was pointed at the crystal. Significant effects were observed only if the evanescent wave of the ATR-IR and the spot point of laser overlapped in space. In a series of experiments, first the background level of the spectrometer was measured with the laser are turned off. Next, the laser is turned on and measurements were taken with 4 s integration time with an IR aperture beam of 8 mm and spectral resolution of 4 cm^{-1} . Results of the measurements with illumination of 50 mW, 90 mW and 130 mW are shown in Fig. 2.

Silicon is often proposed as a photocathode for hydrogen production,^{2,3} because it has a significant photoenergy conversion efficiency in the red portion of the solar spectrum, due to its

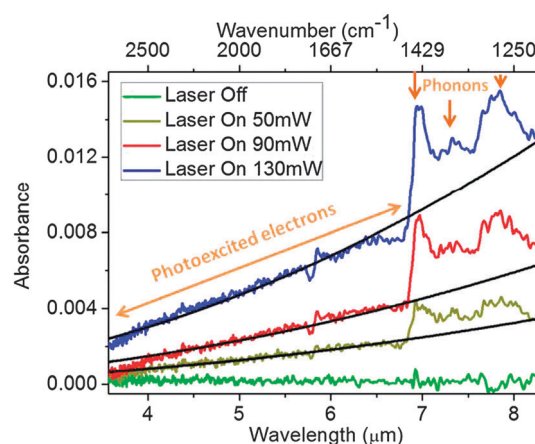


Fig. 2 IR spectroscopy of photoexcited electrons and photoexcited phonons in silicon. Black curves are fits for free carrier absorption.

band gap of 1.1 eV. However, this band gap is not high enough to directly split water, which requires an electrochemical potential of 1.23 eV and some excess energy to allow for over-potentials. Therefore, silicon is usually used in combination with a photoanode, composed of a wide band gap semiconductor material,² to generate a so-called Z scheme. Furthermore, in order to achieve an efficient solar fuel device, it would be advantageous if the silicon surface can be modified with a catalyst. Our ATR-IR technique is thought to become very useful in finding the optimal material for the development of Z-scheme solar fuel systems in the future, because it has the potential to probe not only photoexcitation and thermalization but also surface modifications.

The band gap of silicon of 1.1 eV corresponds to 1.1 μm photon wavelength, *i.e.*, photons with wavelength larger than 1.1 μm (sub-band-gap photons) cannot result in electronic photoexcitation (photoexcitation of electrons), while above-band-gap photons can. That is to say, the photons used in ATR-IR setups are all sub-band-gap photons (MIR photons) and normally electrons in undoped or low-doped silicon (in our case low p-doped, resistivity: $8\text{ }\Omega\text{ cm}$, carrier density: $1.66 \times 10^{15}\text{ cm}^{-3}$) cannot be electronically photoexcited by mid-IR photons.¹³ Electrons photoexcited to the conduction band with above-band-gap photons may become electronically photoexcited for a second time with a second photon, which may even be a sub-band-gap photon. This effect is called free carrier absorption of photoexcited electrons and holes^{7,8,14} (Fig. 1). This process requires the absorption of the two different photons by the same electron, with an extremely low possibility compared to single photon absorption. This kind of photoexcitations is the subject of nonlinear optics, for which two or more photon spectroscopy with a precise optical bench is really needed in the transmission or reflection configuration.⁷⁻⁹ As previously explained, we have observed this effect in our ATR-IR setup.

A photon with an energy higher than the band gap energy of a semiconductor will generate an electron-hole pair. These excited electrons above the band gap of the semiconductor will first relax their excess energy to phonons, which are defined as quantized vibrations of a periodic crystalline lattice in solid materials.⁶ There are four types of phonons in silicon, namely the transverse optical mode (TO), longitudinal optical mode (LO),

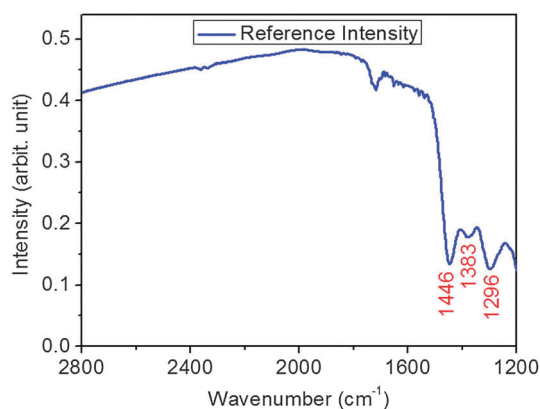


Fig. 3 Reference intensity without any laser.

transverse acoustic mode (TA) and longitudinal acoustic mode (LA).¹⁰ In addition, there are three combinational phonon absorption peaks^{10,15} at 1448 cm^{-1} (3TO), 1378 cm^{-1} (3TO + LO) and 1302 cm^{-1} (2TO + LO). Other sources¹⁵ assign the peaks at 1446 cm^{-1} , 1385 cm^{-1} and 1296 cm^{-1} . With the reduced cut-off wavenumber achieved in our system here, these phonon peaks can be observed. First of all, room temperature phonons can be seen in a background spectrum (Fig. 3 and Fig. SI1–SI3, ESI†). With a spectral resolution of 4 cm^{-1} the phonon peaks appear at 1446 cm^{-1} , 1383 cm^{-1} and 1296 cm^{-1} . Secondly, any change in these phonon peaks can be observed during illumination (Fig. 2). The height of these phonon peaks increases with increasing illumination power (see ESI†).

The peak around 1720 cm^{-1} is assigned to interstitial oxygen (Si–O–Si) vibrations inside the CZ silicon wafer¹⁰ and some other sources¹⁵ assign this peak to a combinational phonon peak. We also observe that the intensity of this peak is increasing with increasing laser power. Some sources¹⁶ claim that the interstitial oxygen (Si–O–Si) impurity traps photoexcited electrons in photovoltaic cells and thereby decreases solar cell performance. The method that we introduce here may be used to understand how the O impurity behaves as a photoexcited electron trap in solar cells.

We also see an increasing slope with increasing light intensity in Fig. 2. This slope is a result of free carrier absorption of photoexcited electrons and holes. In order to fit the free carrier absorption, the wavenumber range from 1500 cm^{-1} to 2800 cm^{-1} (wavelength range $6.66\text{--}3.57\text{ }\mu\text{m}$) is selected, because in this region there is no phonon absorption. Free carrier absorption can be modeled by the Drude model (eqn (1)),^{14,17,18} which states that absorption increases with an increasing number of carriers and with the square of the wavelength

$$\alpha = k\lambda^2 N \quad (1)$$

where α is the absorption coefficient, k is a constant which is a product of all constants in the Drude equation; λ is the wavelength in μm , N is the number of free carriers. The fits for free carrier absorption (for details see ESI†), shown in black color in Fig. 2, not only correlate nicely with the experimental data, but also show the proportionality to the square of the wavelength as expected from the Drude model. The reason for the continuous slope instead of discrete peaks is caused by the interaction between the atomic levels which form

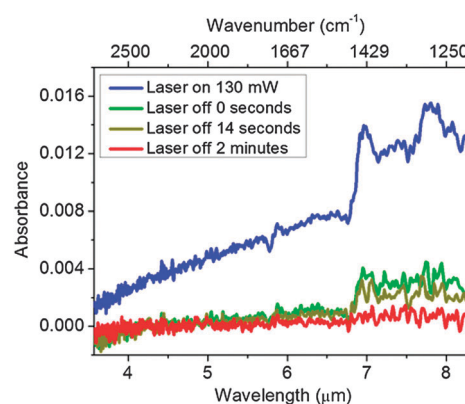


Fig. 4 IR spectroscopy of photoexcited electrons and photoexcited phonons after laser is turned off.

almost continuous bands of discrete states in the bulk solid. The number of silicon atoms present in our crystal can be calculated with the given the dimensions ($2\text{ cm} \times 1.5\text{ cm} \times 500\text{ }\mu\text{m}$), density (2.3290 g cm^{-3}), molar mass ($28.0855\text{ g mol}^{-1}$) and Avogadro constant ($6.022 \times 10^{23}\text{ mol}^{-1}$) which amounts to 5.31×10^{23} atoms. Since the electron orbitals of each of these silicon atoms contribute to the band structure, we conclude that there are 5.31×10^{23} discrete electronic energy levels in our band structure, giving a continuous signal instead of discrete peaks. Fig. 2 shows that the density of free carriers increases with increasing laser power. The increasing slope of the curves with increasing power implies that the density of free carriers is increasing.

Lastly, we decided to evaluate the spectral change for situations with and without laser illumination. We turned off the laser and recorded the spectra for some time after that. The results in Fig. 4 show that the slope of the spectra disappears suddenly but also that the phonon peaks disappear relatively slowly. This is because the relaxation time of the free carriers is much faster than the vibrational phonon relaxation time. In other words, the lifetime of photogenerated phonons is much longer than that of photogenerated electrons. Note that our ATR holder is made of plastic, which is not a good heat conductor. As shown in Fig. 4, it takes about 2 minutes for phonon relaxation in our setup. The relatively long lasting phonon peaks at discrete frequencies and the fast decay of the free carriers at various laser intensities indicate the observation of photoexcitation and thermalization in Si using ATR-IR.

Conclusions

The results show that with our new ATR-IR system, we can detect the absorbance due to photoexcited free carriers and photoexcited phonons in a silicon wafer. This shows that we can measure the two-photon absorption spectrum of Si with ATR-IR. Our results are consistent with absorption that increases quadratically with increasing wavelength. In addition, we showed that phonon absorption and thermalization in silicon can be probed by ATR-IR. These results are important because they show that the classical technique of ATR-IR can be used daily in synthetic labs to probe photon to energy conversion steps inside the semiconductors such as silicon and possibly also ZnSe and CdTe. We believe that this contribution

will have an impact on solar fuel research whose aim is to develop efficient solar to fuel conversion systems.

Thanks to W. L. Vos for use of his facilities and Smartmix Memphis for support. This project was carried out within the research programme of BioSolar Cells, co-financed by the Dutch Ministry of Economic Affairs, Agriculture and Innovation. CINF, Center for Individual Nanoparticle Functionality, is supported by the Danish National Research Foundation.

Notes and references

- 1 N. S. Lewis and D. G. Nocera, *Proc. Natl. Acad. Sci. U. S. A.*, 2006, **103**, 15729–15735.
- 2 H. B. Gray, *Nat. Chem.*, 2009, **1**, 7.
- 3 M. G. Walter, E. L. Warren, J. R. McKone, S. W. Boettcher, Q. X. Mi, E. A. Santori and N. S. Lewis, *Chem. Rev.*, 2010, **110**, 6446–6473.
- 4 R. M. N. Yerga, M. C. A. Galvan, F. del Valle, J. A. V. de la Mano and J. L. G. Fierro, *ChemSusChem*, 2009, **2**, 471–485.
- 5 C. Vigano, J. M. Ruyssehaert and E. Goormaghtigh, *Talanta*, 2005, **65**, 1132–1142.
- 6 J. Shah, *Bull. Am. Phys. Soc.*, 1977, **22**, 702.
- 7 J. Meyer, A. Y. Elezzabi and M. K. Y. Hughes, *IEEE J. Quantum Electron.*, 1995, **31**, 729–734.
- 8 D. Shaughnessy, A. Mandelis, J. Batista, J. Tolev and B. C. Li, *Semicond. Sci. Technol.*, 2006, **21**, 320–334.
- 9 T. G. Euser, P. J. Harding and W. L. Vos, *Rev. Sci. Instrum.*, 2009, **80**, 073104.
- 10 J. W. Medernach, in *Handbook of Vibrational Spectroscopy*, John Wiley & Sons, Ltd, 2006.
- 11 E. Karabudak, S. Schlautmann, H. J. G. E. Gardeniers and G. Mul, *Microfluid. Nanofluid.*, 2012, submitted.
- 12 E. Karabudak, B. L. Mojet, S. Schlautmann, G. Mul and H. J. G. E. Gardeniers, *Anal. Chem.*, 2012, **84**, 3132–3137.
- 13 S. E. Aw, H. S. Tan and C. K. Ong, *J. Phys.: Condens Mater.*, 1991, **3**, 8213–8223.
- 14 D. K. Schroder, R. N. Thomas and J. C. Swartz, *IEEE J. Solid-State Circuits*, 1978, **13**, 180–187.
- 15 M. M. Pradhan, R. K. Garg and M. Arora, *Infrared Phys.*, 1987, **27**, 25–30.
- 16 L. Chen, X. G. Yu, P. Chen, P. Wang, X. Gu, J. G. Lu and D. R. Yang, *Sol. Energy Mater. Sol. Cells*, 2011, **95**, 3148–3151.
- 17 P. Drude, *Ann. Phys.*, 1900, **306**, 566–613.
- 18 P. Drude, *Ann. Phys.*, 1900, **308**, 396–402.